BIOCHEMISTRY
including biophysical chemistry & molecular biology

Article

pubs.acs.org/biochemistry

Structural and Functional Studies on a 3′-Epimerase Involved in the Biosynthesis of dTDP-6-deoxy-D-allose

Rachel L. Kubiak,[†] Rebecca K. Phillips,[†] Matthew W. Zmudka,[†] Melissa R. Ahn,[‡] E. Malaika Maka,[‡] Gwen L. Pyeatt,[‡] Sarah J. Roggensack,[‡] and Hazel M. Holden*[,†]

[†]Department of Biochemistry, University of Wisconsin, Madison, Wisconsin 53706, United States

[‡]Edgewood Campus Middle School, Madison, Wisconsin 53711, United States

Supporting Information

ABSTRACT: Unusual deoxy sugars are often attached to natural products such as antibiotics, antifungals, and chemotherapeutic agents. One such sugar is mycinose, which has been found on the antibiotics chalcomycin and tylosin. An intermediate in the biosynthesis of mycinose is dTDP-6-deoxy-D-allose. Four enzymes are required for the production of dTDP-6-deoxy-D-allose in *Streptomyces bikiniensis*, a soil-dwelling microbe first isolated from the Bikini and Rongelap atolls. Here we describe a combined structural and functional study of the enzyme ChmJ, which reportedly catalyzes the third step in the pathway leading to dTDP-6-deoxy-D-allose formation. Specifically, it has been proposed that ChmJ is a 3′-epimerase that converts dTDP-4-keto-6-deoxyglucose to dTDP-4-keto-6-deoxyallose. This activity, however, has never been verified in vitro. As reported here, we demonstrate using ^{1}H nuclear magnetic resonance that ChmJ, indeed, functions as a 3′-epimerase. In addition, we determined the structure of ChmJ complexed with dTDP-quinovose to 2.0 Å resolution. The structure of ChmJ shows that it belongs to the well-characterized "cupin" superfamily. Two active site residues, His 60 and Tyr 130, were subsequently targeted for study via site-directed mutagenesis and kinetic analyses, and the three-dimensional architecture of the H60N/Y130F mutant protein was determined to 1.6 Å resolution. Finally, the structure of the apoenzyme was determined to 2.2 Å resolution. It has been previously suggested that the position of a conserved tyrosine, Tyr 130 in the case of ChmJ, determines whether an enzyme in this superfamily functions as a mono- or diepimerase. Our results indicate that the orientation of the tyrosine residue in ChmJ is a function of the ligand occupying the active site cleft.

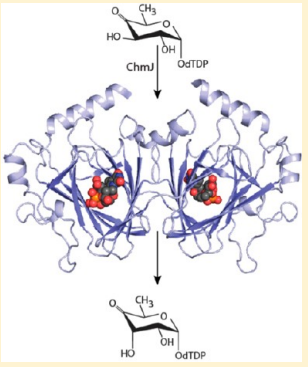

Chalcomycin is a 16-membered natural product that was first isolated in 1962 from *Streptomyces bikiniensis*.[1] It displays significant antibacterial activity against both *Staphylococcus aureus* and *Streptococcus pyogenes*,[2] and also against a number of *Mycoplasma* species.[3] The structure of chalcomycin is shown in Scheme 1,[4] and as can be seen, it belongs to the family of macrolactones that contains 2,3-*trans* double bonds. Attached to the aglycone ring of the drug are two unusual sugars, chalcose and mycinose. Extensive investigations have revealed that the sugar moieties attached to macrolide antibiotics such as chalcomycin often provide or enhance their pharmacological properties.[5] Thus far, three congeners of chalcomycin that differ slightly with respect to the degree of saturation of the aglycone ring or the identity of the substituent attached to the 4″-hydroxyl group of mycinose have been identified.[6,7] In addition to chalcomycin, the unusual sugar mycinose has also been found attached to tylosin, an antibiotic used in veterinary medicine.[8−10]

Scheme 1

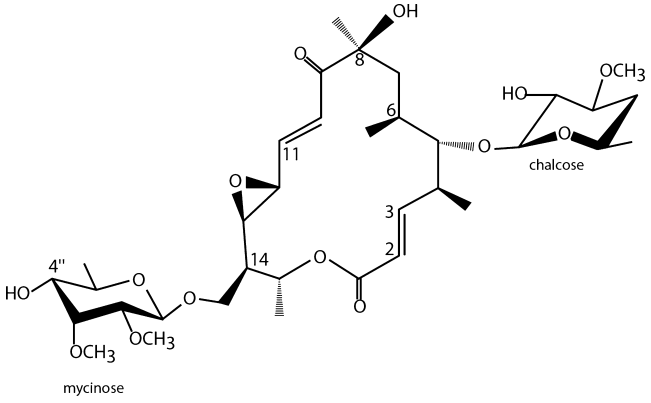

An important intermediate in the biosynthesis of mycinose is dTDP-6-deoxy-D-allose. In *S. bikiniensis*, four enzymes are required for its formation as outlined in Scheme 2.[11] The first two steps, namely, the attachment of glucose 1-phosphate to dTMP followed by the removal of its C-6′ hydroxyl group and oxidation of its C-4′ hydroxyl moiety, are common to many pathways for the production of di-, tri-, and tetradeoxysugars.[12−14] The third step of the pathway, which involves an epimerization about C-3′, is reportedly catalyzed by ChmJ. The final step in dTDP-6-deoxy-D-allose biosynthesis is a reduction of the C-4′ keto group by the action of ChmD.

Received: September 18, 2012
Revised: November 1, 2012
Published: November 1, 2012

dx.doi.org/10.1021/bi3012737 | *Biochemistry* 2012, 51, 9375−9383

Scheme 2

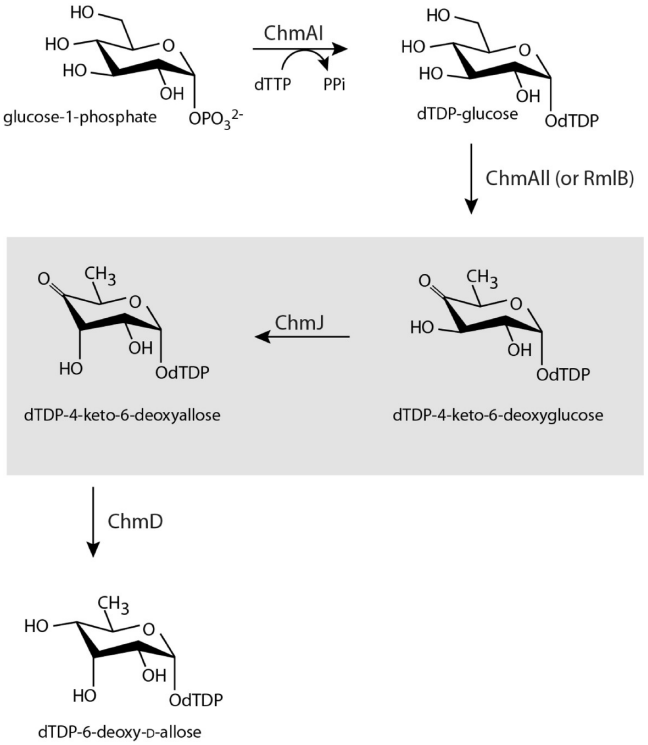

The focus of this investigation is ChmJ, which belongs to a superfamily of sugar epimerases that catalyze reactions about C-3′ or C-5′ of the hexose ring. Some function as mono-epimerases, whereas others catalyze epimerizations about both C-3′ and C-5′ together. Most of our understanding about the structure and function of the 3′,5′-epimerases has been derived from the studies of Naismith and co-workers.[15,16] On the basis of their work, it has been proposed that the protons on C-3′ or C-5′ are abstracted by a strictly conserved histidine residue and that proton donation on the opposite side of the pyranosyl moiety is accomplished by a conserved tyrosine residue. Whereas the 3′,5′-epimerases have been extensively studied, less is known regarding the active site architectures of the 5′-epimerases or 3′-epimerases. The structure of EvaD, a 5′-epimerase, has been determined to high resolution, but in the absence of a nucleotide-linked sugar.[17] By comparing the EvaD structure to that of RmlC, a 3′,5′-epimerase, it was proposed that the orientation of a conserved tyrosine dictates whether a particular enzyme in the superfamily functions as a 5′-epimerase or a 3′,5′-epimerase.[17] Following the structural analysis of EvaD, the molecular architecture of NovW, a 3′-epimerase, was reported.[18,19] As in the case of EvaD, the structure of NovW was determined in the absence of a nucleotide-linked sugar.

In an effort to more fully explore the structure and function of the 3′-epimerases, we initiated a combined X-ray crystallographic and biochemical analysis of ChmJ. For this investigation, the wild-type enzyme structure with bound dTDP-quinovose was determined to 2.0 Å resolution. Three site-directed mutant proteins were subsequently prepared and their kinetic parameters measured (H60N, Y130F, and H60N/Y130F). The H60N/Y130F mutant protein was crystallized and its structure determined to 1.6 Å resolution. Finally, the structure of ChmJ in the absence of bound ligands was determined to 2.2 Å resolution. Taken together, the results of this study provide the first glimpse of a 3′-monoepimerase with a bound dTDP-sugar.

MATERIALS AND METHODS

Cloning, Expression, and Purification of the Wild-Type Enzyme. The *chmJ* gene was amplified via PCR from *S. bikiniensis* (NRRL 2737) genomic DNA using the forward primer 5′-AAA*CATATG*CATCCACTCAGCATCGAGGGG-GCCTGG-3′ and the reverse primer 5′-AAA*CTCGAG*TCTC-TGCGCCTGTTGCTGTTCCTGCC-3′, which added *Nde*I and *Xho*I sites, respectively. The purified PCR product was A-tailed and ligated into the pGEM-T vector (Promega) for screening and sequencing. A pGEM-T-*chmJ* vector construct of the correct sequence was then appropriately digested, and the gene encoding ChmJ was ligated into a pET-31b(+) vector for the production of protein with a C-terminal hexahistidine tag. Rosetta 2 (DE3) *Escherichia coli* cells (Novagen) were transformed with the pET-31-*chmJ* plasmid. Cultures were grown in lysogeny broth medium supplemented with ampicillin and chloramphenicol at 37 °C and subjected to shaking until optical densities of 0.8 at 600 nm were reached. The flasks were then cooled to 16 °C; protein expression was induced with 1 mM isopropyl *β*-D-1-thiogalactopyranoside, and the cells were allowed to grow at 16 °C for an additional 18 h. ChmJ was purified at 4 °C utilizing Ni-nitrilotriacetic acid resin (Qiagen) according to standard procedures. Purified protein was dialyzed against 10 mM Tris (pH 8.0) and 200 mM NaCl. The protein solution was concentrated to approximately 15−20 mg/mL on the basis of an extinction coefficient of 0.59 mL mg^{-1} cm^{-1} at 280 nm and subsequently flash-frozen in liquid nitrogen.

Production of Site-Directed Mutant Proteins. To test the roles of His 60 and Tyr 130 in ChmJ function, three site-directed mutant proteins were constructed: H60N, Y130F, and H60N/Y130F. The mutations were introduced via methods identical or similar to those described within the QuikChange site-directed mutagenesis kit (Stratagene). The H60N mutation was inserted using the forward primer 5′-GCGGCGCGCTG-CGCGGGATCAACTACACCGAGATCCCGCCAGG-3′ and the reverse primer 5′-CCTGGCGGGATCTCGGTGTAGTT-GATCCCGCGCAGCGCGCCGC-3′. The Y130F mutation was inserted using the forward primer 5′-CCGACGACGCC-ACGCTCGTCTTCCTCTGCTCCTCCGGATACGC-3′ and the reverse primer 5′-GCGTATCCGGAGGAGCAGAGGAA-GACGAGCGTGGCGTCGTCGG-3′.

Each mutant protein was expressed and purified in a manner identical to that previously described for the wild-type enzyme. The proteins were dialyzed against 10 mM Tris (pH 8.0) and 200 mM NaCl. Protein concentrations ranged from 13 to 20 mg/mL as measured from the absorbance at 280 nm using an extinction coefficient of 0.59 mL mg^{-1} cm^{-1}. All samples were flash-frozen.

Crystallization and X-ray Data Collection. Crystallization conditions for ChmJ were surveyed by the hanging drop method of vapor diffusion using a sparse matrix screen developed in the laboratory. Diffraction quality crystals of the C-terminal hexahistidine-tagged enzyme at a concentration of 13 mg/mL with 5 mM dTDP-quinovose were grown by mixing in a 1:1 ratio the enzyme solution with 20% poly(ethylene glycol) 3400, 2% 2-methyl-2,4-pentanediol, and 100 mM MOPS (pH 7.0). The dTDP-quinovose sugar was produced as previously described.[20] Note that quinovose is the common name for 6-deoxy-D-glucose and thus represents a substrate analogue for ChmJ.

dx.doi.org/10.1021/bi3012737 | *Biochemistry* 2012, 51, 9375−9383

Table 1. X-ray Data Collection Statistics[a]

	ChmJ−dTDP-quinovose	H60N/Y130F mutant protein	apoenzyme
resolution limits	30−2.0 (2.1−2.0)	30−1.6 (1.66−1.60)	30−1.8 (1.86−1.80)
no. of independent reflections	73347 (9355)	143838 (13940)	100888 (9437)
completeness (%)	94.9 (89.2)	96.1 (93.6)	96.0 (89.3)
redundancy	4.2 (1.8)	4.9 (2.8)	6.7 (2.8)
avg I/avg $\sigma(I)$	8.7 (2.0)	34.8 (3.1)	46.1 (1.7)
R_{sym}[b] (%)	8.8 (31.6)	6.8 (39.4)	7.1 (43.0)

[a]Statistics for the highest-resolution bin are given in parentheses. [b]$R_{sym} = (\sum|I - \bar{I}|/\sum I) \times 100$.

Prior to X-ray data collection, single crystals of the ChmJ−dTDP-quinovose complex were transferred to a synthetic mother liquor containing 15 mM dTDP-quinovose, 18% poly(ethylene glycol) 3400, 200 mM NaCl, 2% 2-methyl-2,4-pentanediol, and 100 mM MOPS (pH 7.0). Subsequently, these crystals were transferred in five steps to a cryoprotectant solution containing 15 mM dTDP-quinovose, 21% poly-(ethylene glycol) 3400, 200 mM NaCl, 2% 2-methyl-2,4-pentanediol, 15% ethylene glycol, and 100 mM MOPS (pH 7.0) and flash-cooled.

High-resolution X-ray data sets were collected at 100 K with a Bruker AXS Platinum 135 CCD detector equipped with Montel optics and controlled by the Proteum software suite. The ChmJ crystals belonged to space group $I4$ with two dimers per asymmetric unit and the following unit cell dimensions: a = b = 140.7 Å, and c = 117.7 Å. The X-ray data sets were processed with SAINT version 7.06A (Bruker AXS Inc.) and internally scaled with SADABS version 2005/1 (Bruker AXS Inc.). Relevant X-ray data collection statistics are listed in Table 1.

Crystals of the H60N/Y130F mutant protein were obtained under conditions similar to those used for the wild-type enzyme, except at pH 6.5 (100 mM MES) and in the presence of 3-methyl-1,5-pentanediol rather than 2-methyl-2,4-pentanediol. The synthetic mother liquor contained 22% poly(ethylene glycol) 3400, 200 mM NaCl, 2% 3-methyl-1,5-pentanediol, ∼20 mM dTDP-4-keto-6-deoxyglucose, and 100 mM MOPS (pH 7.0). The crystals were transferred in five steps to the cryoprotectant solution containing 24% poly(ethylene glycol) 3400, 200 mM NaCl, 2% 3-methyl-1,5-pentanediol, ∼20 mM dTDP-4-keto-6-deoxyglucose, 15% ethylene glycol, and 100 mM MOPS (pH 7.0) and flash-cooled. The dTDP-ketosugar was produced by mixing 300 mM dTDP-glucose with 1 mg/mL RmlB from *E. coli*[21] and 50 mM HEPES (pH 7.5) in an overnight reaction mixture at 25 °C. RmlB was removed using a 10 kDa cutoff Amicon filter, and the resultant dTDP-4-keto-6-deoxyglucose sugar was added to the crystal soaking solutions at a concentration of ∼20 mM. An X-ray data set from a single H60N/Y130F crystal was collected at the Structural Biology Center beamline 19-BM at a wavelength of 0.979 Å (Advanced Photon Source, Argonne National Laboratory, Argonne, IL). The X-ray data set was processed and scaled with HKL3000.[22] Relevant X-ray data collection statistics are listed in Table 1.

To determine the structure of the apoenzyme, the ChmJ−dTDP-quinovose crystals were transferred in five steps to a cryoprotectant solution containing 25% poly(ethylene glycol) 3400, 200 mM NaCl, 2% 2-methyl-2,4-pentanediol, and 15% ethylene glycol and flash-cooled. A complete X-ray data set was collected at the Structural Biology Center beamline 19-BM at a wavelength of 0.979 Å (Advanced Photon Source, Argonne National Laboratory). The X-ray data set was processed and scaled with HKL3000.[22]

Structural Analysis. The initial structure of the ChmJ−dTDP-quinovose complex was determined via molecular replacement with PHASER[23] using the previously determined 4-keto-6-deoxysugar epimerase (NovW) from the novobiocin biosynthetic gene cluster of *Streptomyces sphaeroides*[18] as the search model. The structure was subjected to alternate cycles of manual model building with Coot[24] and refinement with Refmac.[25] Relevant refinement statistics are listed in Table 2.

Table 2. Refinement Statistics

	ChmJ−dTDP-quinovose	H60N/Y130F mutant protein	apoenzyme
space group	$I4$	$I4$	$I4$
unit cell dimensions (Å)	$a = b$ = 140.7, c = 117.7	$a = b$ = 141.0, c = 116.4	$a = b$ = 141.6, c = 115.6
resolution limits (Å)	30−2.0	30−1.6	30−2.2
R factor[a] (overall) (%)/no. of reflections	20.2/73345	21.4/143838	21.7/56511
R factor (working) (%)/no. of reflections	19.9/69652	21.1/136644	21.5/53594
R factor (free) (%)/no. of reflections	24.9/3693	25.4/7194	25.9/2917
no. of protein atoms	6308	6294	6190
no. of heteroatoms	554[b]	615[c]	266[d]
average B value (Å^2)			
protein atoms	23.4	29.1	47.7
ligands	21.8	43.9	−
solvent	24.4	34.0	47.1
weighted root-mean-square deviation from ideality			
bond lengths (Å)	0.009	0.010	0.009
bond angles (deg)	2.2	2.3	2.2
general planes (Å)	0.009	0.009	0.008

[a]R factor = $(\sum|F_o - F_c|/\sum|F_o|) \times 100$, where F_o is the observed structure factor amplitude and F_c is the calculated structure factor amplitude. [b]These include four dTDP-quinovose molecules, seven ethylene glycol molecules, and 386 waters. [c]These include two thymines, two thymidines, four dTDP molecules, 11 ethylene glycols, and 419 waters. [d]These include 12 ethylene glycol molecules, four chloride ions, and 214 waters.

The structures of the double mutant protein and the wild-type apoenzyme were determined by molecular replacement using PHASER and the ChmJ−dTDP-quinovose model as a search probe. The models were rebuilt with Coot[24] and refined with Refmac.[25] Relevant refinement statistics are listed in Table 2.

dx.doi.org/10.1021/bi3012737 | *Biochemistry* 2012, 51, 9375−9383

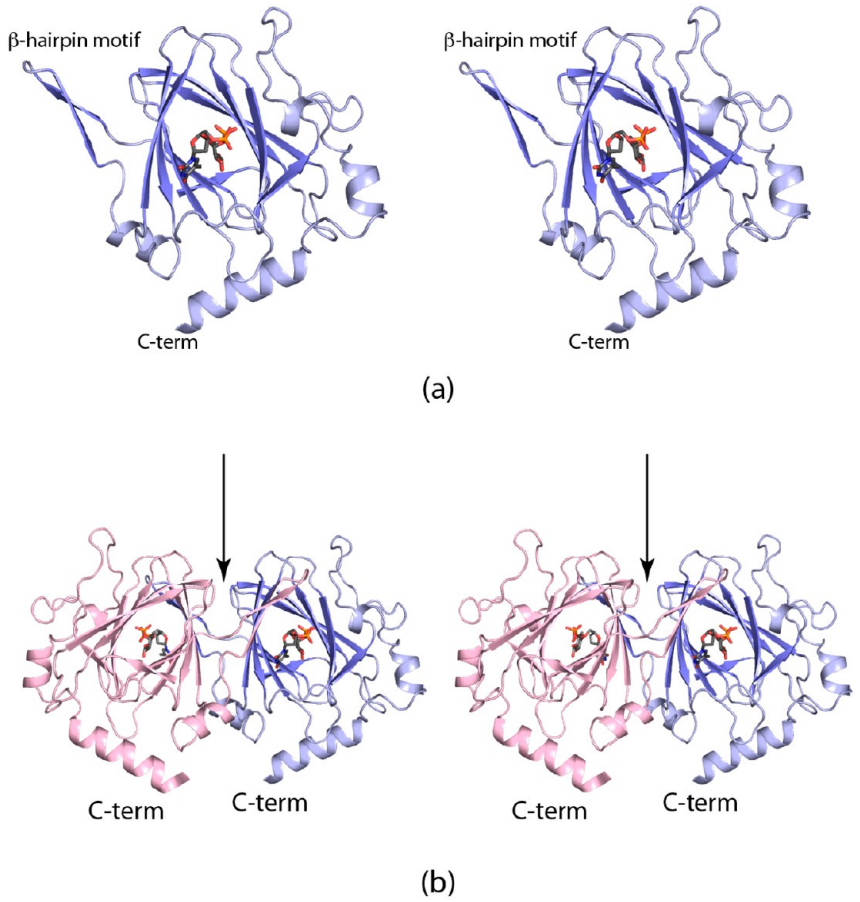

Figure 1. Overall structure of ChmJ. A ribbon representation of one subunit of the ChmJ dimer is shown in panel a. The dTDP-quinovose is displayed as sticks. The complete dimer is shown in panel b. The black arrow indicates the position of the two-fold rotational axis of the dimer. Note how the *β*-hairpin motif of one subunit projects toward the active site of the neighboring subunit. All figures were prepared with PyMOL.[29]

Determination of Kinetic Constants. Steady-state kinetic parameters for ChmJ were determined via a coupled spectrophotometric assay, which followed the conversion of NADPH to $NADP^+$ by the action of ChmD (Scheme 2). The starting material was dTDP-glucose. All reaction mixtures contained 50 mM HEPES (pH 7.5), 2 mM NADPH, 1 mg/mL RmlB, and 1 mg/mL ChmD. The ChmD required for the coupled assay was prepared as described in the next section.

The dTDP-glucose and ChmJ wild-type and mutant protein concentrations varied between reactions as listed below. For the wild-type enzyme, the ChmJ concentration was 0.005 mg/mL in the reaction mixture, with dTDP-glucose concentrations ranging between 0.05 and 12 mM. Both the ChmJ-H60N and ChmJ-Y130F mutant proteins required concentrations of 5 mg/mL, with dTDP-glucose concentrations ranging from 0.1 to 20 mM. The ChmJ double mutant protein required a concentration of 5 mg/mL with dTDP-glucose concentrations varying from 0.1 to 30 mM. The reactions were initiated by the addition of ChmJ and were conducted at 25 °C on a Beckman Coulter DU-640 spectrophotometer for 10 min. Reduction of the dTDP-4-keto-6-deoxyallose sugar and concurrent oxidation of NADPH to $NADP^+$ were monitored by a decrease in absorbance at 340 nm. The data were fit to the equation $v_0 = (V_{max}[S])/(K_M + [S])$. The k_{cat} values were calculated according to the equation $k_{cat} = V_{max}/[E_T]$.

Cloning, Expression, and Purification of ChmD. ChmD was cloned from *S. bikiniensis* genomic DNA using the forward primer 5′-AAA*CATATG*CATCCACTCAGCATCGAGGGGGCCTGG-3′ and the reverse primer 5′-AAA*CTCGAG*CTATCTCTGCGCCTGTTGCTGTTCCTG-3′, which added *Nde*I and *Xho*I sites, respectively. The purified PCR product was A-tailed and ligated into the pGEM-T vector (Promega) for screening and sequencing. A pGEM-T-*chmD* vector construct of the correct sequence was appropriately digested, and the gene encoding ChmD was ligated into a pET28JT vector for the production of the protein with an N-terminal hexahistidine tag.[26] Rosetta 2 (DE3) *E. coli* cells (Novagen) were transformed with the pET28JT-*chmD* plasmid. Cultures were grown in terrific broth medium supplemented with kanamycin and chloramphenicol at 37 °C and subjected to shaking until optical densities of 0.8 were reached at 600 nm. The flasks were then cooled to 24 °C, and cell growth was continued for 20 h. The cells were subsequently induced with 50 μM IPTG and allowed to express the protein at 24 °C for an additional 18 h. ChmD was purified at 4 °C utilizing Ni-nitrilotriacetic acid resin (Qiagen) according to standard procedures. The purified protein was then dialyzed against 10 mM Tris (pH 8.0), 500 mM NaCl, and 10% glycerol. The protein preparation was concentrated to approximately 20 mg/mL using an extinction coefficient of 1.22 mL mg^{-1} cm^{-1} at 280 nm and subsequently flash-frozen in liquid nitrogen.

Preparation of the ChmJ–ChmD Product and Analysis by ^{1}H NMR. A large-scale reaction was run to produce the dTDP-sugar product produced by the combined action of ChmJ and ChmD. The mixture included 10 mM dTDP-glucose, 15 mM NADPH, 0.5 mg/mL RmlB, 0.5 mg/mL

dx.doi.org/10.1021/bi3012737 | *Biochemistry* 2012, 51, 9375–9383

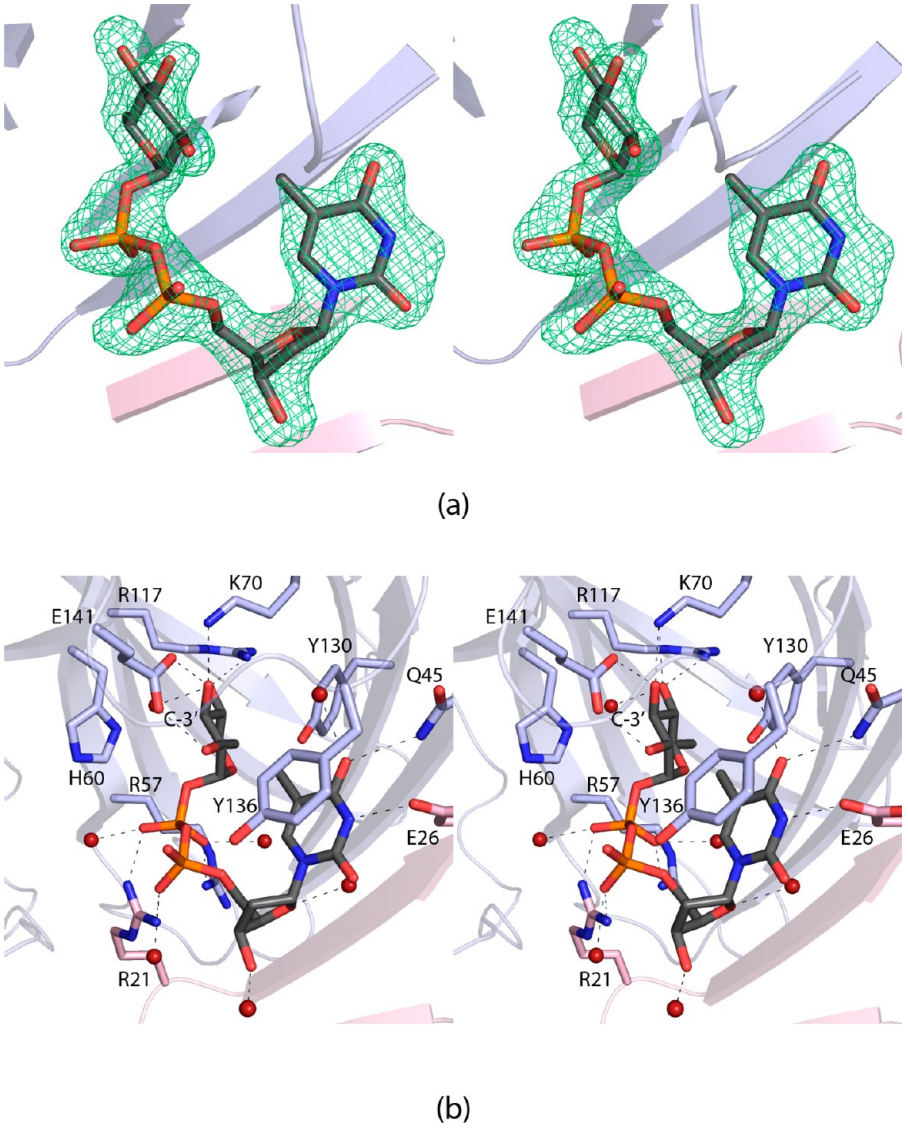

Figure 2. Active site of ChmJ. The electron density corresponding to the bound dTDP-quinovose ligand is displayed in panel a. The map, contoured at 2σ, was calculated with coefficients of the form $F_o - F_c$, where F_o was the native structure factor amplitude and F_c was the calculated structure factor amplitude. Those amino acid residues or solvent molecules lying within 3.2 Å of dTDP-quinovose are shown in panel b. Residues from subunit 1 and subunit 2 are colored light blue and pink, respectively. The black dashed lines indicate potential hydrogen bonds.

ChmJ, 0.5 mg/mL ChmD, and 50 mM HEPES (pH 7.5). The reaction was run at 24 °C for approximately 16 h. The sample was passed through a 10 kDa cutoff filter (Amicon) to remove the enzymes, and the filtrate was diluted 1:9 with water. The reaction mixture was analyzed via an ÄKTA Purifier high-performance liquid chromatography system (GE Healthcare) equipped with a Resource-Q 6 mL anion exchange column (GE Healthcare). The dTDP-sugar product was separated from the other reaction components using a 90 mL linear gradient from 0 to 700 mM ammonium acetate (pH 4.0) run at a rate of 6 mL/min. The peak corresponding to the dTDP-sugar product was collected and the sample lyophilized. Its identity as dTDP-6-deoxyallose was confirmed by electrospray ionization mass spectrometry (Mass Spectrometry/Proteomic Facility at the University of Wisconsin) with a parent ion at m/z 547 and ^{1}H NMR spectroscopy (Nuclear Magnetic Resonance Facility, University of Wisconsin). The observed NMR values were in agreement with those previously determined for dTDP-6-deoxyallose.[27] Specifically, the small $J_{1'',2''}$ coupling constant (3.7 Hz) and the relatively small $J_{2'',3''}$ coupling constant (<7 Hz) of the hexose ring indicate an equatorially disposed $H_{1''}$ proton, an axially disposed $H_{2''}$ proton, and an equatorially disposed $H_{3''}$ proton. Additionally, the small $J_{3'',4''}$ coupling constant (3.1 Hz) and the large $J_{4'',5''}$ coupling constant (10.1 Hz) of the hexose ring reveal that the compound possesses an axially disposed $H_{4''}$ and an axially disposed $H_{5''}$ proton: ^{1}H NMR (750 MHz, D_2O) δ 7.55 (s, 1H, H_6), 6.17 (t, 1H, $H_{1'}$, J = 6.9 Hz), 5.33 (dd, 1H, $H_{1''}$, J = 6.9, 3.7 Hz), 4.44 (m, 1H, $H_{3'}$), 4.01−3.99 (m, 3H, $H_{4'}$ and $H_{5'}$), 3.93 (m, 1H, $H_{5''}$, J = 10.1, 6.2 Hz), 3.90 (m, 1H, $H_{3''}$, J < 5 Hz), 3.60 (m, 1H, $H_{2''}$, J < 7 Hz), 3.20 (dd, 1H, $H_{4''}$, J = 10.1, 3.1 Hz), 2.19 (dd, 1H, $H_{2'}$, J = 13.5, 6.9 Hz), 2.17 (dd, 1H, $H_{2'}$, J = 13.0, 3.7 Hz), 1.17 (s, 3H, H_7), 1.10 (d, 3H, $H_{6''}$, J = 6.2 Hz).

RESULTS AND DISCUSSION

Structure of ChmJ in Complex with dTDP-quinovose. ChmJ is dimeric with each subunit containing 196 amino acid residues.[11] For our initial analysis, the ChmJ structure was

dx.doi.org/10.1021/bi3012737 | *Biochemistry* 2012, 51, 9375−9383

Table 3. Kinetic Parameters

protein	K_m (mM)	k_{cat} (s^{-1})	k_{cat}/K_m (M^{-1} s^{-1})
wild type	0.4 ± 0.07	6.4 ± 0.24	1.0×10^5
H60N	0.4 ± 0.05	$(2.7 \pm 0.83) \times 10^{-3}$	7.2
Y130F	0.7 ± 0.1	$(3.9 \pm 0.18) \times 10^{-3}$	5.7
H60N/Y130F	0.7 ± 0.08	$(4.4 \pm 0.12) \times 10^{-3}$	6.1

determined in the presence of dTDP-quinovose to 2.0 Å resolution and refined to an *R* factor of 20.2%. dTDP-quinovose differs from the natural ChmJ substrate by having a hydroxyl group rather than a keto moiety at the C-4′ position (Scheme 2). The polypeptide chain backbones for the four monomers in the asymmetric unit were very well ordered with no breaks from the N- to C-termini. Indeed, the Ramachandran statistics were excellent, with 91.2 and 8.8% of the ϕ and ψ values lying within the core and allowed regions of the plot, respectively. The α-carbons for the two dimers in the asymmetric unit superimpose upon one another with a root-mean-square deviation of 0.25 Å. Given the close structural correspondence between each subunit, the following discussion refers only to the first chain (or in some cases dimer) in the X-ray coordinate file.

Shown in Figure 1a is a ribbon representation of one subunit of ChmJ. Its overall architecture is dominated by two layers of antiparallel β-sheet that form a flattened β-barrel. One layer contains six strands, whereas the second consists of five. The β-barrel is decorated on the outside by four helical regions and a two-stranded antiparallel β-sheet. This β-hairpin motif extends toward the second subunit of the dimer as illustrated in Figure 1b. Because of this domain swapping, the six-stranded β-sheets in each subunit are extended to eight strands, and residues contributed from both subunits form the active sites. The overall fold exhibited by ChmJ places it into the well-characterized cupin superfamily.[28] The name of the superfamily is derived from the Latin term "*cupa*", which means "small barrel". Members demonstrate a wide range of biological functions ranging from enzymes to transcription factors to storage proteins in plant seeds.[28]

Shown in Figure 2a is the electron density corresponding to the bound dTDP-quinovose. The density shows that the hexose adopts the $^4C_1$ chair conformation and that it is attached to the nucleotide moiety via an axial linkage. A close-up view of the ChmJ active site is provided in Figure 2b. The nucleoside portion of the ligand sits near the surface of the subunit, whereas the pyranosyl group projects into the β-barrel. The aromatic side chain of Tyr 136 forms a parallel stacking interaction with the thymine ring of the dTDP-sugar. Both the side chains of Gln 45 (subunit 1) and Glu 26 (subunit 2) lie within 3.2 Å of the thymine ring. The guanidinium groups of Arg 57 (subunit 1) and Arg 21 (subunit 2) surround the phosphoryl oxygens of the ligand. The hexose moiety is situated within hydrogen bonding distance of the side chains of Lys 70, Arg 117, and Glu 141. Numerous well-ordered water molecules surround the dTDP-quinovose ligand. The side chains of His 60 and Tyr 130 are positioned at 3.7 and 4.1 Å, respectively, from C-3′ of the hexose. There are three cis peptides in ChmJ: Ile 59, Pro 65, and Pro 66. Of these, only Ile 59 is located in the active site region.

Functional Analysis of ChmJ. Although annotated as a 3′-epimerase, the actual enzymatic activity of ChmJ has never been verified in vitro. To prove that ChmJ functions as a monoepimerase, we set up a reaction mixture containing dTDP-glucose, NADPH, RmlB, ChmJ, and ChmD (Scheme 2). The product of the pathway was purified and subjected to both mass spectrometry and ^{1}H NMR (Supporting Information). The data from the mass spectrometry yielded a parent ion at *m*/*z* 547, which is the appropriate mass for dTDP-6-deoxy-D-allose. More importantly, the ^{1}H NMR data revealed that in the product, the protons on C-2′, C-3′, C-4′, and C-5′ were oriented in the axial, equatorial, axial, and axial positions, respectively, as would be expected for a monoepimerized product (Scheme 2). It was not possible to analyze the ChmJ product directly by NMR because of its instability arising from the C-4′ keto moiety. Reduction of the ChmJ product by ChmD resulted in a stable nucleotide-linked sugar whose identity could be verified by NMR.

For the 3′,5′-epimerases, it has been proposed that an active site histidine serves as the catalytic base to abstract the protons from C-3′ and C-5′, resulting in C-4′ enolate intermediates.[15,16] It has also been suggested that a tyrosine on the opposite side of the sugar functions as the active site acid to reprotonate C-3′ and C-5′.[15,16] In ChmJ, these residues correspond to His 60 and Tyr 130, respectively. To test the roles of these residues in

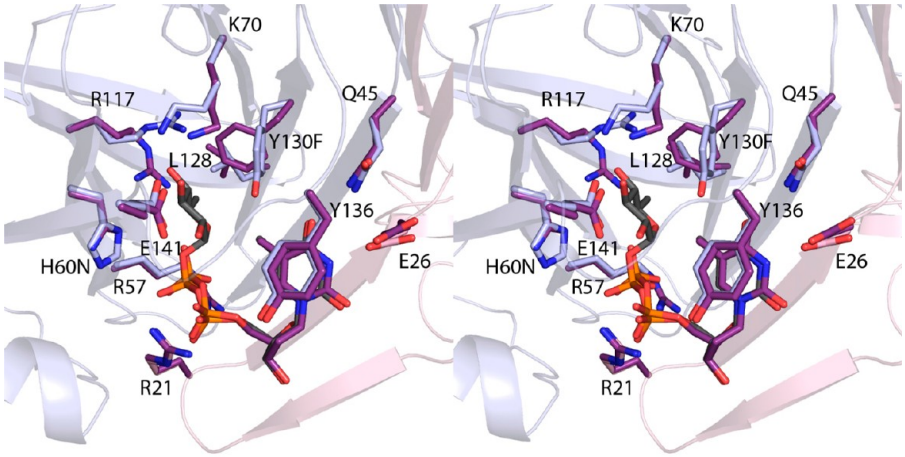

Figure 3. Superposition of the active sites for the wild-type enzyme and the H60N/Y130F mutant protein. Side chains for the wild-type enzyme are highlighted in light blue and pink, whereas those for the double mutant protein are displayed in purple. The only significant movement of side chains occurs near the Y130F mutation.

dx.doi.org/10.1021/bi3012737 | *Biochemistry* 2012, 51, 9375−9383

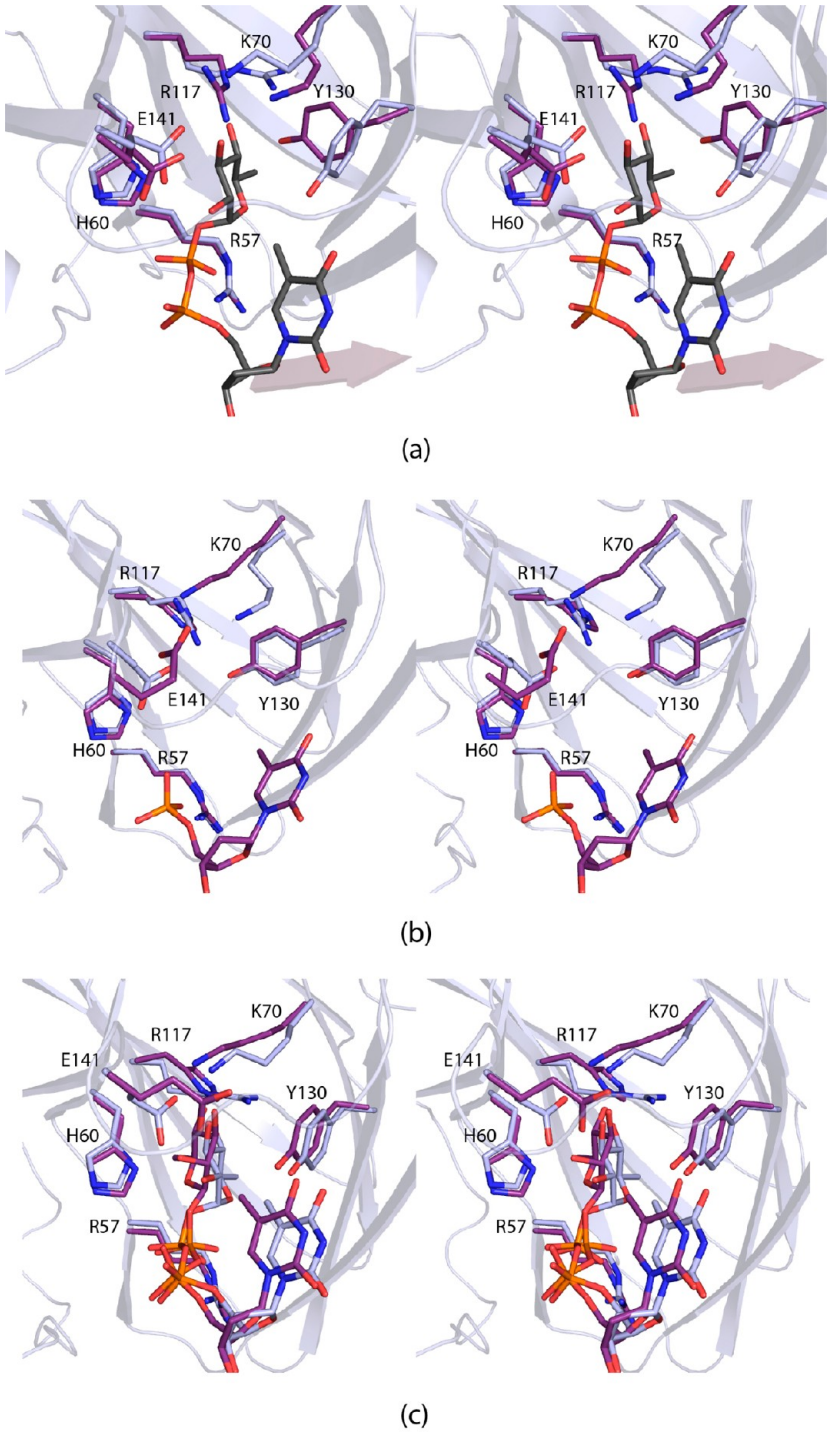

Figure 4. Movement of the conserved tyrosine is most likely a function of the identity of the ligand bound in the active site. A superposition of the active sites of ChmJ, with or without bound dTDP-sugar, is displayed in panel a. The ChmJ structure complexed with dTDP-quinovose is colored blue, whereas the model of the enzyme lacking a bound ligand is colored purple. In panel b, the active sites of ChmJ without a bound ligand and EvaD with dTMP are superimposed. ChmJ and EvaD are colored light blue and purple, respectively. Coordinates for EvaD were from Protein Data Bank entry 1OI6. Shown in panel c is a superposition of ChmJ (light blue) and RmlC (purple), both with bound dTDP-sugars. Coordinates for RmlC were from Protein Data Bank entry 2IXC.

catalysis, three site-directed mutant proteins were constructed (H60N, Y130F, and H60N/Y130F), and their steady-state kinetic parameters determined via a coupled spectrophotometric assay, which follows the conversion of NADPH to $NADP^+$ by the action of ChmD as described in Materials and Methods.

For the assays, the ChmJ substrate was synthesized in situ. This was done out of necessity because of the instability of its substrate. As such, several controls were conducted to confirm that RmlB (Scheme 2) and ChmD (Scheme 2 , used for monitoring the reaction progress), along with NADPH, were at saturating concentrations and were not rate-limiting. For each control reaction, the concentrations of these enzymes or

dx.doi.org/10.1021/bi3012737 | *Biochemistry* 2012, 51, 9375−9383

NADPH were individually doubled whereas all other conditions were kept identical to those described in Materials and Methods. The reactions were monitored for 10 min, and the rates were linear throughout the time course. No changes in rates were observed for any of the control reactions as compared to the original values, indicating that both the enzymes and NADPH were at saturating concentrations.

Whereas the apparent substrate K_m values for the mutant proteins were similar to that observed for the wild-type protein, the catalytic efficiencies of these enzymes were significantly impaired (Table 3). As proposed for other sugar epimerases, His 60 most likely serves as the catalytic base and Tyr 130 as the proton donor (Figure 2b).

Structural Analysis of the Double Mutant Protein. We subsequently crystallized and determined the three-dimensional structure of the H60N/Y130F mutant protein to ensure that the catalytic impairment was due to the loss of functional side chains, rather than large conformational changes. Although the H60N/Y130F mutant protein crystals were soaked in the presence of dTDP-4-keto-6-deoxyglucose sugar, only dTDP was observed bound in the active site according to the electron density maps calculated with $F_o - F_c$ coefficients. dTDP-4-keto-6-deoxyglucose is notoriously unstable, and most likely, dTDP was a contaminant or breakdown product in the sample utilized in the studies.

A superposition of the active sites for the wild-type and H60N/Y130F mutant proteins is presented in Figure 3. Changing His 60 to an asparagine residue resulted in virtually no three-dimensional perturbation within the region surrounding the mutation. The situation is different for the Y130F mutation. The phenylalanine side chain in the mutant protein swings toward the side chains of Arg 117 and Leu 128, which in turn adopt different conformations to accommodate this movement. It is possible that the alternate conformation of the phenylalanine side chain is a function of the observation that only dTDP, rather than a dTDP-sugar, was bound in the active site. Other than these few changes, the double mutation had little effect on the overall conformation of ChmJ, such that the α-carbons for the wild-type and double mutant protein subunits correspond with a root-mean-square deviation of 0.19 Å.

Structural Analysis of the Apoenzyme. There has been speculation in the literature regarding those factors that distinguish diepimerases from monoepimerases. By comparing the structures of the 3′,5′-epimerase from *Streptococcus suis*, (RmlC), and the 5′-epimerase from *Amycolatopsis orientalis*, (EvaD), it was proposed that the position of the tyrosine in the active site region determines whether an enzyme functions as a mono- or di-epimerase.[17] The problem with this analysis, however, was that the comparison was made between the structure of RmlC complexed with a dTDP-linked sugar and the structure of EvaD with only bound dTMP.

We were curious about whether the conformation of the tyrosine is simply dependent upon the presence or absence of a pyranosyl moiety in the active site. Accordingly, crystals of the ChmJ−dTDP-quinovose complex were soaked in synthetic solutions lacking the nucleotide-linked sugar. An X-ray data set from an apoenzyme crystal was subsequently collected to 2.2 Å resolution, and the structural model was refined to an R factor of 21.5%.

Shown in Figure 4a is a superposition of the active site regions for ChmJ, with or without dTDP-quinovose. The tyrosine adopts alternate conformations depending upon the presence or absence of a bound ligand. A superposition of the ChmJ apoenzyme structure and the EvaD−dTMP complex model is presented in Figure 4b. ChmJ functions as a 3′-monoepimerase, whereas EvaD is a 5′-monoepimerase. As can be seen, the active site tyrosines adopt similar positions. Importantly, in both of these models, a pyranosyl moiety is missing in the active site. A superposition of the structures of RmlC and ChmJ, both with bound dTDP-sugars ligands, is provided in Figure 4c. Clearly, the active site tyrosines adopt similar conformations even though RmlC is a diepimerase and ChmJ is a monoepimerase. It is possible that had the structure of EvaD been determined in the presence of a dTDP-sugar, the conformation of its tyrosine would have been similar to that observed for the RmlC−dTDP-sugar and the ChmJ−dTDP-sugar complexes.

In conclusion, we have established that ChmJ is a 3′-epimerase as previously predicted by amino acid sequence comparisons.[11] On the basis of both structural and kinetic analyses, it can be concluded that His 60 and Tyr 130 play key roles in the catalytic mechanism of the enzyme. Importantly, by comparing the structures of ChmJ with or without a bound dTDP-sugar ligand, it is clear that the conserved tyrosine adopts one of two alternative conformations depending upon whether a ligand is or is not bound in the active site region. These studies highlight the danger of assigning function to sugar epimerases based solely on X-ray structures, and in particular on the position of this residue in the absence of a substrate or substrate analogue. The observed orientation of the tyrosine residue in a sugar epimerase may have nothing to do with whether it functions as a mono- or diepimerase but rather is a function of what is occupying the active site.

■ ASSOCIATED CONTENT

Supporting Information

Results from mass spectroscopy and ^{1}H NMR analysis of the ChmJ−ChmD product, namely dTDP-6-deoxyallose (Figures S1 and S2). This material is available free of charge via the Internet at http://pubs.acs.org.

Accession Codes

X-ray coordinates have been deposited in the Research Collaboratory for Structural Bioinformatics (Protein Data Bank entries 4HMZ, 4HN0, and 4HN1).

■ AUTHOR INFORMATION

Corresponding Author

*E-mail: hazel_holden@biochem.wisc.edu. Fax: (608) 262-1319. Phone: (608) 262-4988.

Funding

This research was supported in part by National Science Foundation (NSF) Grant MCB-0849274 to H.M.H. and NSF Predoctoral Fellowships DGE-0718123 to R.L.K. and DGE-0718123 to R.K.P.

Notes

The authors declare no competing financial interest.

■ ACKNOWLEDGMENTS

We thank Professor Grover Waldrop for helpful discussions. This research was conducted as part of Project CRYSTAL, an outreach program for middle school students supported by the National Science Foundation (http://www.projectcrystal.org/). A portion of the research described in this paper was performed at Argonne National Laboratory, Structural Biology Center at

the Advanced Source (U.S. Department of Energy, Office of Biological and Environmental Research, under Contract DE-AC02-06CH11357). We gratefully acknowledge Dr. Norma E. C. Duke for assistance during the X-ray data collection at Argonne.

■ ABBREVIATIONS

dTDP, thymidine diphosphate; dTMP, thymidine monophosphate; HEPES, *N*-(2-hydroxyethyl)piperazine-*N*′-2-ethanesulfonic acid; MES, 2-(*N*-morpholino)ethanesulfonic acid; MOPS, 3-(*N*-morpholino)propanesulfonic acid; NADPH, reduced nicotinamide adenine dinucleotide phosphate; NMR, nuclear magnetic resonance; PCR, polymerase chain reaction; Tris, tris(hydroxymethyl)aminomethane.

■ REFERENCES

(1) Frohardt, R. P., Pitillo, R. F., and Ehrlich, J. (1962) Chalcomycin and its fermentative production. U.S. Patent 3,065,137.

(2) Coffey, G. L., Anderson, L. E., Douros, J. D., Erlandson, A. L., Jr., Fisher, M. W., Hans, R. J., Pittillo, R. F., Vogler, D. K., Weston, K. S., and Ehrlich, J. (1963) Chalcomycin, a new antibiotic: Biological studies. *Can. J. Microbiol. 9*, 665−669.

(3) Omura, S., Hironaka, Y., Nakagawa, A., Umezawa, I., and Hata, T. (1972) Antimycoplasma activities of macrolide antibiotics. *J. Antibiot. 25*, 105−108.

(4) Woo, P. W. K., and Rubin, J. R. (1996) Chalcomycin: Single-crystal X-ray crystallographic analysis; biosynthetic and stereochemical correlations with other polyoxo macrolide antibiotics. *Tetrahedron 52*, 3857−3872.

(5) Weymouth-Wilson, A. C. (1997) The role of carbohydrates in biologically active natural products. *Nat. Prod. Rep. 14*, 99−110.

(6) Kim, S. D., Ryoo, I. J., Kim, C. J., Kim, W. G., Kim, J. P., Kong, J. Y., Koshino, H., Uramoto, M., and Yoo, I. D. (1996) GERI-155, a new macrolide antibiotic related to chalcomycin. *J. Antibiot. 49*, 955−957.

(7) Goo, Y. M., Lee, Y. Y., and Kim, B. T. (1997) A new 16-membered chalcomycin type macrolide antibiotic, 250-144C. *J Antibiot. 50*, 85−88.

(8) Fouces, R., Mellado, E., Diez, B., and Barredo, J. L. (1999) The tylosin biosynthetic cluster from *Streptomyces fradiae*: Genetic organization of the left region. *Microbiology 145* (Part 4), 855−868.

(9) Bate, N., and Cundliffe, E. (1999) The mycinose-biosynthetic genes of *Streptomyces fradiae*, producer of tylosin. *J. Ind. Microbiol. Biotechnol. 23*, 118−122.

(10) Anadon, A., and Reeve-johnson, L. (1999) Macrolide antibiotics, drug interactions and microsomal enzymes: Implications for veterinary medicine. *Res. Vet. Sci. 66*, 197−203.

(11) Ward, S. L., Hu, Z., Schirmer, A., Reid, R., Revill, W. P., Reeves, C. D., Petrakovsky, O. V., Dong, S. D., and Katz, L. (2004) Chalcomycin biosynthesis gene cluster from *Streptomyces bikiniensis*: Novel features of an unusual ketolide produced through expression of the chm polyketide synthase in *Streptomyces fradiae*. *Antimicrob. Agents Chemother. 48*, 4703−4712.

(12) Thibodeaux, C. J., Melancon, C. E., and Liu, H. W. (2007) Unusual sugar biosynthesis and natural product glycodiversification. *Nature 446*, 1008−1016.

(13) Thibodeaux, C. J., Melancon, C. E., III, and Liu, H. W. (2008) Natural-product sugar biosynthesis and enzymatic glycodiversification. *Angew. Chem., Int. Ed. 47*, 9814−9859.

(14) White-Phillip, J., Thibodeaux, C. J., and Liu, H. W. (2009) Enzymatic synthesis of TDP-deoxysugars. *Methods Enzymol. 459*, 521−544.

(15) Naismith, J. H. (2004) Chemical insights from structural studies of enzymes. *Biochem. Soc. Trans. 32*, 647−654.

(16) Dong, C., Major, L. L., Srikannathasan, V., Errey, J. C., Giraud, M. F., Lam, J. S., Graninger, M., Messner, P., McNeil, M. R., Field, R. A., Whitfield, C., and Naismith, J. H. (2007) RmlC, a C3′ and C5′ carbohydrate epimerase, appears to operate via an intermediate with an unusual twist boat conformation. *J. Mol. Biol. 365*, 146−159.

(17) Merkel, A. B., Major, L. L., Errey, J. C., Burkart, M. D., Field, R. A., Walsh, C. T., and Naismith, J. H. (2004) The position of a key tyrosine in dTDP-4-keto-6-deoxy-D-glucose-5-epimerase (EvaD) alters the substrate profile for this RmlC-like enzyme. *J. Biol. Chem. 279*, 32684−32691.

(18) Jakimowicz, P., Tello, M., Meyers, C. L., Walsh, C. T., Buttner, M. J., Field, R. A., and Lawson, D. M. (2006) The 1.6-Å resolution crystal structure of NovW: A 4-keto-6-deoxy sugar epimerase from the novobiocin biosynthetic gene cluster of *Streptomyces sphaeroides*. *Proteins 63*, 261−265.

(19) Tello, M., Jakimowicz, P., Errey, J. C., Freel Meyers, C. L., Walsh, C. T., Buttner, M. J., Lawson, D. M., and Field, R. A. (2006) Characterisation of *Streptomyces sphaeroides* NovW and revision of its functional assignment to a dTDP-6-deoxy-D-xylo-4-hexulose 3-epimerase. *Chem. Commun.*, 1079−1081.

(20) Kubiak, R. L., and Holden, H. M. (2011) Combined structural and functional investigation of a C-3″-ketoreductase involved in the biosynthesis of dTDP-L-digitoxose. *Biochemistry 50*, 5905−5917.

(21) Hegeman, A. D., Gross, J. W., and Frey, P. A. (2001) Probing catalysis by *Escherichia coli* dTDP-glucose-4,6-dehydratase: Identification and preliminary characterization of functional amino acid residues at the active site. *Biochemistry 40*, 6598−6610.

(22) Otwinowski, Z., and Minor, W. (1997) Processing of X-ray diffraction data collected in oscillation mode. *Methods Enzymol. 276*, 307−326.

(23) McCoy, A. J., Grosse-Kunstleve, R. W., Adams, P. D., Winn, M. D., Storoni, L. C., and Read, R. J. (2007) Phaser crystallographic software. *J. Appl. Crystallogr. 40*, 658−674.

(24) Emsley, P., and Cowtan, K. (2004) Coot: Model-building tools for molecular graphics. *Acta Crystallogr. D60*, 2126−2132.

(25) Murshudov, G. N., Vagin, A. A., and Dodson, E. J. (1997) Refinement of macromolecular structures by the maximum-likelihood method. *Acta Crystallogr. D53*, 240−255.

(26) Thoden, J. B., Timson, D. J., Reece, R. J., and Holden, H. M. (2005) Molecular structure of human galactokinase: Implications for type II galactosemia. *J. Biol. Chem. 280*, 9662−9670.

(27) Thuy, T. T., Liou, K., Oh, T. J., Kim, D. H., Nam, D. H., Yoo, J. C., and Sohng, J. K. (2007) Biosynthesis of dTDP-6-deoxy-β-D-allose, biochemical characterization of dTDP-4-keto-6-deoxyglucose reductase (GerKI) from *Streptomyces* sp. KCTC 0041BP. *Glycobiology 17*, 119−126.

(28) Dunwell, J. M., Culham, A., Carter, C. E., Sosa-Aguirre, C. R., and Goodenough, P. W. (2001) Evolution of functional diversity in the cupin superfamily. *Trends Biochem. Sci. 26*, 740−746.

(29) DeLano, W. L. (2002) *The PyMOL Molecular Graphics System*, DeLano Scientific, San Carlos, CA.